Sohag Journal of Sciences
An International Journal

A numerical solution of 2-D single-phase-lag (SPL) bio-heat model using alternating direction implicit (ADI) finite difference method

Ibrahim Abbas, Aboelnour Abdalla, Fathi Anwar* and Hussien Sapoor

*Mathematics Department, Faculty of Science, Sohag University, Sohag, Egypt.

Received: 5 Augt. 2022, Revised: 29 Augt. 2022, Accepted: 29 Aug. 2022.
Published online: 1 Sept.. 2022

Abstract:
Background Here, the two-dimensional single-phase-lag (SPL) bioheat transfer model in biological tissue by considering the heat conduction law is introduced. The formulated SPL bioheat model is an extension of the bioheat transfer models proposed by Pennes, Cattaneo-Vernotte, and Tzou. Through this model, the thermal properties of living tissues, as well as the temperature distribution in living tissues, and the estimated resulting thermal damage due to laser irradiation are studied. The effects of delay time, blood perfusion, metabolism, and laser parameters on the spread of heat in the body and the resulting thermal damage are studied. Also, comparisons have been made between the results from the SPL and Pennes bio-heat models as well as the resulting thermal damage. The results of the SPL bio-heat model have been compared with previous results. The used numerical method is the (ADI) finite difference method. The proposed ADI difference scheme is unconditionally stable. The results have been presented graphically and discussed in detail.

Keywords: ADI finite difference; delay time; Laser Radiation; thermal damage; SPL Bioheat transfer.

1. Introduction

Due to the difficulty of measuring in-vivo, the thermal properties of living tissue are only approximately known, and this is because the thermal properties of the tissue can be changed because of necropsy, and as well, there won't be perfusion effects in the tissue that is analyzed outside of the body. To measure thermal properties in-vivo, there are a number of methods, and each gives a different outcome. So far, to measure the thermal properties of in-vivo tissue, there is no clear way. Many therapeutic approaches entail the control of heat transfer mechanisms in the body. Thermic therapeutics lead to freezing or superheating tumors in the body. Ideally, only the diseased cell is damaged, not the surrounding healthy tissue. Understanding how the tissue will thermally respond would allow physicians to plan treatment doses and durations prior to the procedure [1]. Numerous conditions are associated with the temperature response of tissue and blood perfusion, for example, diabetes, skin grafts, and frostbite. All of these conditions are affected by the amount of blood flow that is supplied to an area. Before problems occur, proper treatment could be applied quickly and effectively if the thermal properties of the affected tissue could be watched exactly. On account of their heterogeneous internal structure, heat transfer analysis is difficult and complicated in living tissues.

The process of heat transfer in living tissues involves perfusion through capillary tubes within the tissues, convection between blood and tissue, heat conduction in solid tissue matrix and blood vessels, metabolic heat generation, and evaporation, etc. Pennes' [2] bioheat transfer model, which is based on Fourier's law of heat conduction, is used to simulate heat transfer in living biological tissue:

$$q(\mathbf{r},t) = -k\nabla T(\mathbf{r},t) \quad (1)$$

where $\nabla T(\mathbf{r},t)$ is the temperature gradient, k is the thermal conductivity, and $q(\mathbf{r},t)$ is the local heat flux. Pennes' model was widely used in studying tissue heat transfer due to its simplicity. However, there are some drawbacks to Pennes' model considering it is built upon the classical Fourier's law, which supposes that the propagation speed of thermal disturbance is unlimited. Even though this hypothesis is sensible in most practical applications, it does not succeed in certain thermal conditions. Because temperature alternation (an unusual oscillation of tissue temperature with heating) and wave-like behavior are many a time noticed, the non-homogeneous inner structure of biological tissue [3] suggests the existence of non-Fourier heat conduction behavior. Firstly, Richardson et al. [4] have noticed the temperature oscillation in living tissue. And later, Roemer et al. [5] exposed the thigh muscle of a dog to an abrupt application of microwave heating at different power levels. Thereafter, four different

* Corresponding author E-mail: fathianwur@yahoo.com
© 2022 Sohag University

experiments with processed meat for different boundary conditions were carried out by Mitra et al.[6] and also noted the wave-like behavior. At the same time, Davydov et al. [7] have discovered experimentally that the standard Fourier-theory based heat diffusion model cannot explain the heat transfer in muscle tissue. Banerjee et al. [8] discovered that the hyperbolic non-Fourier heat conduction equation is more effective than the equivalent Fourier heat conduction formula experimentally by laser irradiation of meat. Other models have been proposed to solve the paradox in Pennes' model. Cattaneo [9] and Vernotte [10] used Fourier law to determine the C-V major relation, which is given as:

$$q(\mathbf{r}, t + \tau_q) = -k\nabla T(\mathbf{r}, t) \tag{2}$$

where τ_q is relaxation time because of heat flow. C–V model supposes that temperature gradient and heat flow occur at the same position at various times. The delay time between the heat flux and the temperature gradient is known as the relaxation time and thermalization time. S, Wahyudi et al. [11] studied the Pennes bioheat model by using a finite difference scheme. Zhao et al. [12] used the finite difference method to investigate the one-dimensional Pennes' bioheat model. Patil et al. [13] have used the finite-difference scheme-based analysis of bioheat transfers in human breast cysts. Kabiri A. and Talaee M.R. [14] used the Eigenvalue method to solve a one-dimensional hyperbolic Pennes bioheat equation with a moving heat source. Kabiri A. and Talaee M.R. [15] used the Pennes model for analysis of the thermal field and tissue damage resulting from moving the laser in cancer thermal therapy. Using the Pennes model, a Monte Carlo simulation of the photo-thermal cancer therapy of melanin has been conducted [16]. Abdalla et al. [17] applied the finite difference method to study the effects of fractional derivatives of the bio-heat model on living tissues. A Non-Fourier bioheat model for bone grinding with application to skull base neurosurgery has been studied by Kabiri A. and Talaee M.R. [18]. Hobiny and Abbas [19] have studied the fractional-order bioheat transfer model. . Over the last decades many problems have been solved by generalized thermoelastic theories as in [20-24]. The ADI-FD method was introduced by Namiki [25] and Zheng et al. [26, 27], and it is an unconditionally stable method. It allows Δt to be increased, which can result in substantial reductions in the total execution time of numerical problems.

In the present paper, we examine a 2-D SPL bioheat transfer model to analyze the resulting thermal damage from laser radiation in biological tissue. We resort to the numerical scheme to solve the 2-D SPL bio-heat transfer model for analyzing the temperature variations in biological tissue. We analyzed the critical effect of relaxation time. The effect of the unevenness of other parameters on the temperature profile in living skin tissue is discussed in detail.

2. Mathematical formulation of problem

By virtue of [9, 28], the chief equation of the single-phase lag bio-heat model (SPL) in biological tissues is defined as:

$$k\left(\frac{\partial^2 T}{\partial x^2} + \frac{\partial^2 T}{\partial y^2}\right) = \left(1 + \tau_q \frac{\partial}{\partial t}\right)\left(\rho c \frac{\partial T}{\partial t} - Q_b - Q_m - Q_{ext}\right) \tag{3}$$

where t and τ_q are defined respectively by the time and the phase lag of the heat flux density. T is the tissue temperature. ρ is the density of the mass of tissues, k is the tissue thermal conductivity, c is the tissues specific heat, and the heat source of blood perfusion is denoted by Q_b which is expressed as:

$$Q_b = \omega_b \rho_b c_b (T_b - T) \tag{4}$$

Where T_b is the blood temperature, ρ_b is the density of the mass of blood, c_b is the specific heat of blood, the rate of blood perfusion is denoted by ω_b, and Q_m is denote to the heat generated by metabolic mechanisms because of different physiological operations that occur in the remainder of the body. Due to Mitchell et al. [29], the metabolically generated heat can define as:

$$Q_m = Q_{mo} \times 2^{\beta\left(\frac{T - T_o}{10}\right)} \tag{5}$$

Where β is the constant associated metabolic, Q_{mo} is the reference metabolic heating resource, and T_o denoted to the initial temperature of local tissue, The dependences on metabolic heating generation can be generally estimated as linear functions of the temperature of local tissue as below

$$Q_m = Q_{mo}\left(1 + \beta\left(\frac{T - T_o}{10}\right)\right) \tag{6}$$

Where Q_{ext} represent the heat generated from the heating source per unit volume of tissue, which is submitted by [30] as a laser heating source and determined as:

$$Q_{ext}(x, y, t) = I_o \mu_a [H(a - |y|)]\left[u(t) - u(t - \tau_p)\right]\left[C_1 e^{-\frac{k_1}{\Delta} x} - C_2 e^{-\frac{k_2}{\Delta} x}\right] \tag{7}$$

Where H is a Heaviside function; k_1, C_1, k_2, and C_2 are the diffuse reflectance function of R_d which is given in [30]; $u(t)$ is the unit step functions; I_o is the density of laser; τ_p the time of tissue exposure to the laser; Δ is permeation depth; and μ_a is the absorption coefficients. The permeation depth was clarified by [30] as:

© 2022 Sohag University

$$\Delta = \frac{1}{\sqrt{3\mu_a(\mu_a + \mu_s(1-g))}} \quad (8)$$

Where g is the anisotropy factor and μ_s the scattering coefficient. Currently, initial conditions and boundary conditions can be described by:

$$T(x,y,0) = T_b, \qquad \frac{\partial T(x,y,0)}{\partial t} = 0 \quad (9)$$

3. Solution of the problem

In this section, we present the basic ideas for a numerical solution to the main equation (3). On problem the domain of space and time are $x \in [0,L], y \in \left[-\frac{P}{2}, \frac{P}{2}\right], t \in [0, t_f]$.

We discretization these domains uniformly as a set of nodes points (x_i, y_j, t_k), such as $x_i = ih, i = 0,1,2,\dots,I$, $y_j = jg, j = 0,1,2,\dots,J$ and $t_k = kp, k = 0,1,2,\dots,K$. Therefore, $p = \Delta t = \frac{t_f}{N} > 0$, $g = \Delta y = \frac{P}{M} > 0$, $h = \Delta x = \frac{L}{M} > 0$. To solve main equation (4) we use the alternating direction implicit finite difference method (ADI-FDM), which is divided into two main steps such that if we have temperature T at any (k) time step, we can get T at $\left(k + \frac{1}{2}\right)$ time step using the first step of ADI, and we get T at the time step $(k+1)$ using the second step of ADI. By using the approximations of finite-difference Seen below:

$$\frac{\partial T}{\partial t} = \frac{T_{i,j}^{k+\frac{1}{2}} - T_{i,j}^{k}}{\frac{p}{2}} + O(p),$$
$$\frac{\partial^2 T}{\partial t^2} = \frac{T_{i,j}^{k-\frac{1}{2}} - 2T_{i,j}^{k} + T_{i,j}^{k+\frac{1}{2}}}{\frac{p^2}{4}} + O(p^2) \quad (12)$$

$$\frac{\partial T}{\partial x} = \frac{T_{i+1,j}^{k} - T_{i-1,j}^{k}}{2h} + O(h),$$
$$\frac{\partial^2 T}{\partial x^2} = \frac{T_{i-1,j}^{k} - 2T_{i,j}^{k} + T_{i+1,j}^{k}}{h^2} + O(h^2) \quad (13)$$

$$\frac{\partial T}{\partial y} = \frac{T_{i,j+1}^{k+\frac{1}{2}} - T_{i,j-1}^{k+\frac{1}{2}}}{2g} + O(g),$$
$$\frac{\partial^2 T}{\partial y^2} = \frac{T_{i,j-1}^{k+\frac{1}{2}} - 2T_{i,j}^{k+\frac{1}{2}} + T_{i,j+1}^{k+\frac{1}{2}}}{g^2} + O(g^2) \quad (14)$$

$$-k\frac{\partial T(0,y,t)}{\partial x} = 0, \qquad -k\frac{\partial T(L,y,t)}{\partial x} = 0 \quad (10)$$

$$-k\frac{\partial T(x,y_{int},t)}{\partial y} = 0, \qquad -k\frac{\partial T(x,y_f,t)}{\partial y} = 0 \quad (11)$$

by some arranging the first ADI step of the chief equation (3) can be written as:

$$\lambda T_{i,j-1}^{k+\frac{1}{2}} + \lambda^* T_{i,j}^{k+\frac{1}{2}} + \lambda T_{i,j+1}^{k+\frac{1}{2}} = -\mu T_{i-1,j}^{k} + \mu^* T_{i,j}^{k} - \mu T_{i+1,j}^{k} + C T_{i,j}^{k-\frac{1}{2}} + \Theta_{i,j}^{k} \quad (15)$$

where

$$\lambda = \frac{k}{g^2}, \mu = \frac{k}{h^2}, C = \frac{4\rho c t_q}{p^2},$$
$$\lambda^* = -2\lambda - \frac{4\rho c t_q}{p^2} - \frac{2}{p}\left(\rho c + t_q \omega_b \rho_b c_b - \frac{t_q Q_{mo}\beta}{10}\right)$$
$$\mu^* = 2\mu - \frac{8\rho c t_q}{p^2} + \omega_b \rho_b c_b - \frac{Q_{mo}\beta}{10} - \frac{2}{p}\left(\rho c + t_q \omega_b \rho_b c_b - \frac{t_q Q_{mo}\beta}{10}\right)$$
$$\Theta_{i,j}^{k} = \frac{T_o Q_{mo}\beta}{10} - \omega_b \rho_b c_b T_b - Q_{mo} - (Q_{ext})_{i,j}^{k}$$

Equation (15) is called the first ADI step. Using initial and boundary conditions in equations (9), (10), and (11). Equation (15) represent system of linear equations.

$$\begin{bmatrix} M & 2\lambda & & & & \\ \lambda & M & \lambda & & & \\ & \lambda & M & \lambda & & \\ & & \ddots & \ddots & \ddots & \\ & & & \lambda & M & \lambda \\ & & & & 2\lambda & M \end{bmatrix} \left(\begin{bmatrix} T_{0,0} & \cdots & T_{0,J-1} & T_{0,J} \\ T_{1,0} & \cdots & T_{1,J-1} & T_{1,J} \\ T_{2,0} & \cdots & T_{2,J-1} & T_{2,J} \\ \vdots & \vdots & \vdots & \vdots \\ T_{I-2,0} & \cdots & T_{I-2,J-1} & T_{I-2,J} \\ T_{I-1,0} & \cdots & T_{I-1,J-1} & T_{I-1,J} \\ T_{I,0} & \cdots & T_{I,J-1} & T_{I,J} \end{bmatrix}^{\frac{1}{2}} \right)^{T} \quad (16)$$

$$= \begin{bmatrix} \mu^* & -2\mu & & & & \\ -\mu & \mu^* & -\mu & & & \\ & -\mu & \mu^* & -\mu & & \\ & & \ddots & \ddots & \ddots & \\ & & & -\mu & \mu^* & -\mu \\ & & & & -2\mu & \mu^* \end{bmatrix} \begin{bmatrix} T_{0,0} & \cdots & T_{0,J-1} & T_{0,J} \\ T_{1,0} & \cdots & T_{1,J-1} & T_{1,J} \\ T_{2,0} & \cdots & T_{2,J-1} & T_{2,J} \\ & \vdots & \vdots & \vdots \\ T_{I-2,0} & \cdots & T_{I-2,J-1} & T_{I-2,J} \\ T_{I-1,0} & \cdots & T_{I-1,J-1} & T_{I-1,J} \\ T_{I,0} & \cdots & T_{I,J-1} & T_{I,J} \end{bmatrix}^0 + \begin{bmatrix} \Theta_{0,0} & \cdots & \Theta_{0,J-1} & \Theta_{0,J} \\ \Theta_{1,0} & \cdots & \Theta_{1,J-1} & \Theta_{1,J} \\ \Theta_{2,0} & \cdots & \Theta_{2,J-1} & T_{2,J} \\ & \vdots & \vdots & \vdots \\ \Theta_{I-2,0} & \cdots & \Theta_{I-2,J-1} & \Theta_{I-2,J} \\ \Theta_{I-1,0} & \cdots & \Theta_{I-1,J-1} & \Theta_{I-1,J} \\ \Theta_{I,0} & \cdots & \Theta_{I,J-1} & \Theta_{I,J} \end{bmatrix}^0$$

Where $M = \lambda^* - C$ and $i = 0,1,2,\dots,I$. then for $k = 1,2,\dots,K$.

$$\begin{bmatrix} \lambda^* & 2\lambda & & & & \\ \lambda & \lambda^* & \lambda & & & \\ & \lambda & \lambda^* & \lambda & & \\ & & \ddots & \ddots & \ddots & \\ & & & \lambda & \lambda^* & \lambda \\ & & & & 2\lambda & \lambda^* \end{bmatrix} \left(\begin{bmatrix} T_{0,0} & \cdots & T_{0,J-1} & T_{0,J} \\ T_{1,0} & \cdots & T_{1,J-1} & T_{1,J} \\ T_{2,0} & \cdots & T_{2,J-1} & T_{2,J} \\ & \vdots & \vdots & \vdots \\ T_{I-2,0} & \cdots & T_{I-2,J-1} & T_{I-2,J} \\ T_{I-1,0} & \cdots & T_{I-1,J-1} & T_{I-1,J} \\ T_{I,0} & \cdots & T_{I,J-1} & T_{I,J} \end{bmatrix}^{k+\frac{1}{2}} \right)^T$$

$$= \begin{bmatrix} \mu^* & -2\mu & & & & \\ -\mu & \mu^* & -\mu & & & \\ & -\mu & \mu^* & -\mu & & \\ & & \ddots & \ddots & \ddots & \\ & & & -\mu & \mu^* & -\mu \\ & & & & -2\mu & \mu^* \end{bmatrix} \begin{bmatrix} T_{0,0} & \cdots & T_{0,J-1} & T_{0,J} \\ T_{1,0} & \cdots & T_{1,J-1} & T_{1,J} \\ T_{2,0} & \cdots & T_{2,J-1} & T_{2,J} \\ & \vdots & \vdots & \vdots \\ T_{I-2,0} & \cdots & T_{I-2,J-1} & T_{I-2,J} \\ T_{I-1,0} & \cdots & T_{I-1,J-1} & T_{I-1,J} \\ T_{I,0} & \cdots & T_{I,J-1} & T_{I,J} \end{bmatrix}^k$$

$$+C \begin{bmatrix} T_{0,0} & \cdots & T_{0,J-1} & T_{0,J} \\ T_{1,0} & \cdots & T_{1,J-1} & T_{1,J} \\ T_{2,0} & \cdots & T_{2,J-1} & T_{2,J} \\ & \vdots & \vdots & \vdots \\ T_{I-2,0} & \cdots & T_{I-2,J-1} & T_{I-2,J} \\ T_{I-1,0} & \cdots & T_{I-1,J-1} & T_{I-1,J} \\ T_{I,0} & \cdots & T_{I,J-1} & T_{I,J} \end{bmatrix}^{k-\frac{1}{2}} + \begin{bmatrix} \Theta_{0,0} & \cdots & \Theta_{0,J-1} & \Theta_{0,J} \\ \Theta_{1,0} & \cdots & \Theta_{1,J-1} & \Theta_{1,J} \\ \Theta_{2,0} & \cdots & \Theta_{2,J-1} & T_{2,J} \\ & \vdots & \vdots & \vdots \\ \Theta_{I-2,0} & \cdots & \Theta_{I-2,J-1} & \Theta_{I-2,J} \\ \Theta_{I-1,0} & \cdots & \Theta_{I-1,J-1} & \Theta_{I-1,J} \\ \Theta_{I,0} & \cdots & \Theta_{I,J-1} & \Theta_{I,J} \end{bmatrix}^k$$

And the second ADI step of the chief equation (3) can be written as:

$$\xi T_{i-1,j}^{k+1} + \xi^* T_{i,j}^{k+1} + \xi T_{i+1,j}^{k+1} = -\alpha T_{i,j-1}^{k+\frac{1}{2}} + \alpha^* T_{i,j}^{k+\frac{1}{2}} - \alpha T_{i,j+1}^{k+\frac{1}{2}} + C T_{i,j}^{k} + \Theta_{i,j}^{k} \quad (17)$$

where

$$\xi = \frac{k}{h^2}, \xi^* = -2\xi - \frac{4\rho c t_q}{p^2} - \omega_b \rho_b c_b + \frac{Q_{mo}\beta}{10} - \frac{2}{p}\left(\rho c + t_q \omega_b \rho_b c_b - \frac{t_q Q_{mo}\beta}{10}\right)$$

$$\alpha = \frac{k}{g^2}, C = \frac{4\rho c t_q}{p^2}, \alpha^* = 2\alpha - \frac{8\rho c t_q}{p^2} - \frac{2}{p}\left(\rho c + t_q \omega_b \rho_b c_b - \frac{t_q Q_{mo}\beta}{10}\right)$$

$$\Theta_{i,j}^{k} = \frac{T_o Q_{mo}\beta}{10} - \omega_b \rho_b c_b T_b - Q_{mo} - (Q_{ext})_{i,j}^{k}$$

Equation (17) is called the first ADI step. Using initial and boundary conditions in equations (9), (10), and (11). Equation (17) represent system of linear equations.

© 2022 Sohag University

$$\begin{bmatrix} \xi^* & 2\xi & & & & \\ \xi & \xi^* & \xi & & & \\ & \xi & \xi^* & \xi & \ddots & \\ & & \ddots & \ddots & \xi^* & \xi \\ & & & \xi & 2\xi & \xi^* \end{bmatrix} \begin{bmatrix} T_{0,0} & \cdots & T_{0,J-1} & T_{0,J} \\ T_{1,0} & \cdots & T_{1,J-1} & T_{1,J} \\ T_{2,0} & \cdots & T_{2,J-1} & T_{2,J} \\ \vdots & \vdots & \vdots & \vdots \\ T_{I-2,0} & \cdots & T_{I-2,J-1} & T_{I-2,J} \\ T_{I-1,0} & \cdots & T_{I-1,J-1} & T_{I-1,J} \\ T_{I,0} & \cdots & T_{I,J-1} & T_{I,J} \end{bmatrix}^{k+1}$$

$$= \begin{bmatrix} \alpha^* & -2\alpha & & & & \\ -\alpha & \alpha^* & -\alpha & & & \\ & -\alpha & \alpha^* & -\alpha & \ddots & \\ & & \ddots & -\alpha & \alpha^* & -\alpha \\ & & & & -2\alpha & \alpha^* \end{bmatrix} \left(\begin{bmatrix} T_{0,0} & \cdots & T_{0,J-1} & T_{0,J} \\ T_{1,0} & \cdots & T_{1,J-1} & T_{1,J} \\ T_{2,0} & \cdots & T_{2,J-1} & T_{2,J} \\ \vdots & \vdots & \vdots & \vdots \\ T_{I-2,0} & \cdots & T_{I-2,J-1} & T_{I-2,J} \\ T_{I-1,0} & \cdots & T_{I-1,J-1} & T_{I-1,J} \\ T_{I,0} & \cdots & T_{I,J-1} & T_{I,J} \end{bmatrix}^{k+\frac{1}{2}} \right)^{T} \tag{18}$$

$$+C \begin{bmatrix} T_{0,0} & \cdots & T_{0,J-1} & T_{0,J} \\ T_{1,0} & \cdots & T_{1,J-1} & T_{1,J} \\ T_{2,0} & \cdots & T_{2,J-1} & T_{2,J} \\ \vdots & \vdots & \vdots & \vdots \\ T_{I-2,0} & \cdots & T_{I-2,J-1} & T_{I-1,J} \\ T_{I-1,0} & \cdots & T_{I-1,J-1} & T_{I-1,J} \\ T_{I,0} & \cdots & T_{I,J-1} & T_{I,J} \end{bmatrix}^{k} + \begin{bmatrix} \Theta_{0,0} & \cdots & \Theta_{0,J-1} & \Theta_{0,J} \\ \Theta_{1,0} & \cdots & \Theta_{1,J-1} & \Theta_{1,J} \\ \Theta_{2,0} & \cdots & \Theta_{2,J-1} & T_{2,J} \\ \vdots & \vdots & \vdots & \vdots \\ \Theta_{I-2,0} & \cdots & \Theta_{I-2,J-1} & \Theta_{I-2,J} \\ \Theta_{I-1,0} & \cdots & \Theta_{I-1,J-1} & \Theta_{I-1,J} \\ \Theta_{I,0} & \cdots & \Theta_{I,J-1} & \Theta_{I,J} \end{bmatrix}^{k}$$

4. Numerical computation and Analysis

In that study, the variation of temperature in living tissues has examined under the hyperbolic Pennes bioheat model has been founded with the interface and suitable boundary conditions. The perfusion, metabolic and conducting heat resource terms have been used in the formulations [31-34]. And has been chosen idealistic values of heat characteristics in living tissues for the numerical computations [35]

$$\rho_b = 1060(\mathrm{kg})(\mathrm{m}^{-3}), \rho = 1000(\mathrm{kg})(\mathrm{m}^{-3}),$$
$$c_b = 3860\ (\mathrm{J})(\mathrm{kg}^{-1})(\mathrm{k}^{-1}), K_2 = 1.63e^{3.4R_d},$$
$$\omega_b = 3.87 \times 10^{-3}\ (\mathrm{s}^{-1}),\ T_b = T_o = 37\ ^{\circ}\mathrm{C},$$
$$I_o = 122 \times 10^3\ (\mathrm{W})(\mathrm{m}^{-2}), \tau_p = 15(\mathrm{s}),$$
$$c = 4187\ (\mathrm{J})(\mathrm{kg}^{-1})(\mathrm{k}^{-1}), L = P = 0.05(\mathrm{m}),$$
$$Q_m = 1.19 \times 10^3(\mathrm{W})(\mathrm{m}^{-3}), g = 0.9,$$
$$C_1 = 3.09 + 5.44R_d - 2.12e^{-21.5R_d},$$
$$C_2 = 2.09 - 1.47R_d - 2.12e^{-21.5R_d},$$
$$K_1 = 1 - \left(1 - \frac{1}{\sqrt{3}}\right)e^{-20.1R_d}, R_d = 0.05,$$
$$\mu_s = 12000\ (\mathrm{m}^{-1}), \mu_a = 40(\mathrm{m}^{-1}),$$
$$k = 0.628\ (\mathrm{W})(\mathrm{m}^{-1})(\mathrm{k}^{-1}).$$

In the biological applied sciences in living tissue, the rigorous diagnosis of burn is one of the main features, It is a fundamental part of the thermal therapy. Moritz and Henriques [36, 37] developed a method that is used to measure thermal damages. The non-dimensional quantity of thermal damages Ω can be determined by

$$\Omega = \int_0^t B \exp\left(-\frac{E_a}{RT}\right) dt \tag{12}$$

Where $B = 3.1 \times 10^{98}(s^{-1})$ is the frequency factor, $R = 8.314\ \mathrm{J/(mal\ k)}$ is the constant of universal gas, and $E_a = 6.27 \times 10^5\ \mathrm{J/mal}$ the activation energy. Again a modified thermal damage model has been developed by Dombrovsky and Timchenko[38], so it can be written as:

$$\frac{d\Omega}{dt} = A(1-\Omega)\exp\left(-\frac{E_a}{RT}\right) - Bw_b\Omega;$$
$$\text{at } t = 0, \quad \frac{d\Omega}{dt} = 0 \tag{20}$$

The results here are predicated on the skin tissues with the aforesaid attributes, In addition to the blood parameters and laser attributes. MATLAB(R2020a) software have been utilized in making the computations and the results are given graphically in Figures 1–10.

Figures 1-4 shows the effect of delay time on the distribution of temperature over the distance at $t = 60s$, the time histories of surface temperature at

$x = y = 0$, as well as thermal damage occurring to the surface of the skin along with time. where in Pennes model $(t_q = 0)$ and $(t_q = 16s)$ in SPL models.

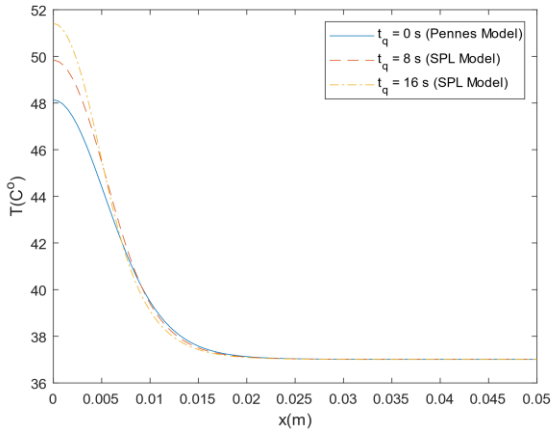

Fig. 1: The distribution of temperature over the distance at $t = 60$ s according to Pennes and SPL bio-heat models.

Fig. 2: The time histories of surface temperature at $x = y = 0$ according to Pennes and SPL bio-heat m models.

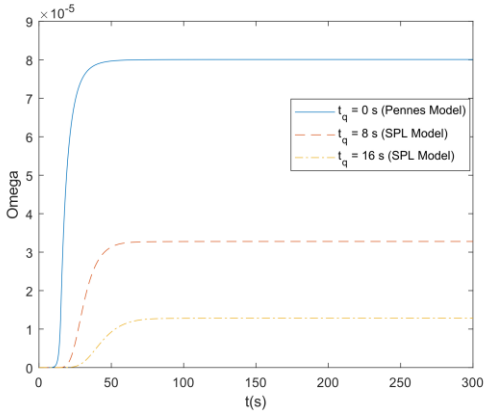

Fig. 3. The estimated thermal damage occurring to the surface of the skin along with time according to Pennes and SPL bio-heat models.

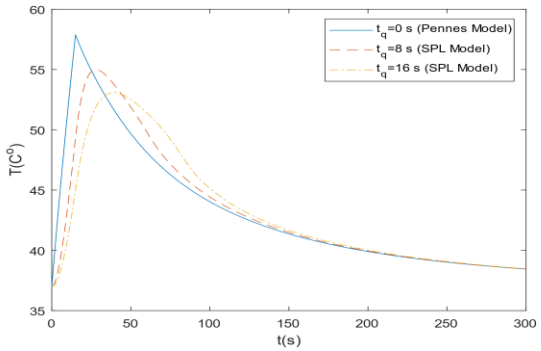

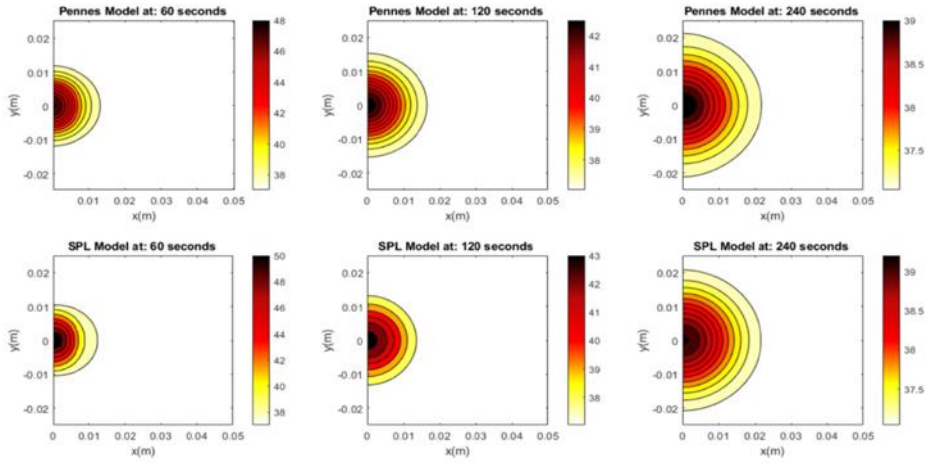

Fig. 4: Contour plots of the temperature variations along with the changes in space at different times according to Pennes and SPL bio-heat models.

Figures 5-8 display the effect of the rate of the blood perfusion on the distribution of temperature over the distance at $t = 60s$, as well as the time histories of surface temperature at $x = 0$. It is clear that the higher the blood flow rate, the lower the temperature and thermal damage. When the laser is applied to the

© 2022 Sohag University

skin, this leads to a rise in the temperature of the skin, which makes the body need to cool itself, and the process of vasodilation occurs so that the blood vessels under your skin get wider. This increases blood flow to the skin where it is cooler away from the warm inner body. This lets the body release heat through heat radiation which decreases the resulting thermal damage. In rats or men, increased temperature causes an exponential increase in perfusion[3, 39].

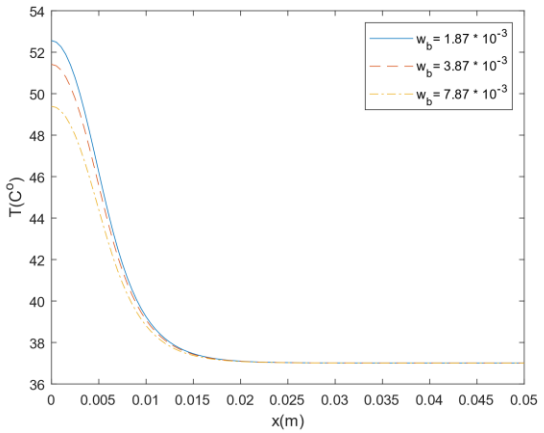

Fig. 5. The effect of the rate of the blood perfusion on the distribution of temperature over the distance at $t = 60$ s and $y = 0$ according to SPL bio-heat model.

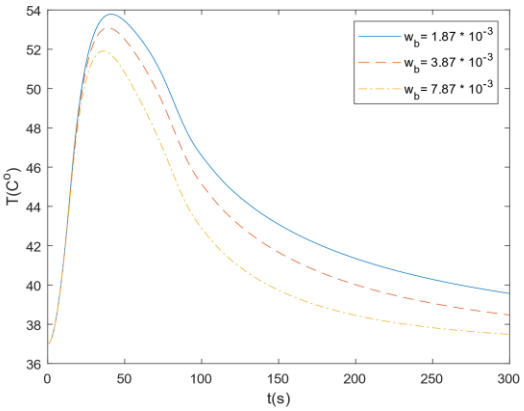

Fig. 6: The effect of the rate of the blood perfusion on the time histories of surface temperature at $x = y = 0$ according to SPL bio-heat model.

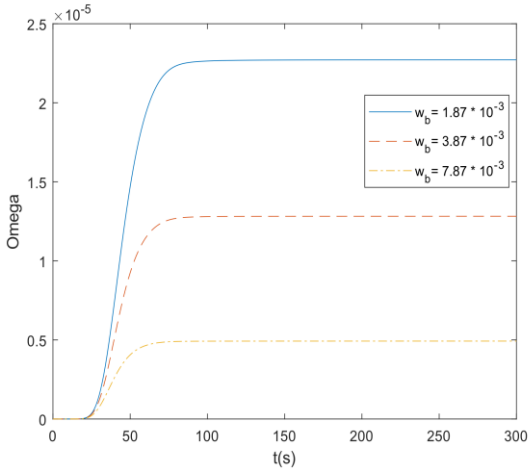

Fig. 7: The effect of the rate of the blood perfusion on the thermal damage occurring to the surface of the skin at $y = 0$ according to SPL bio-heat model.

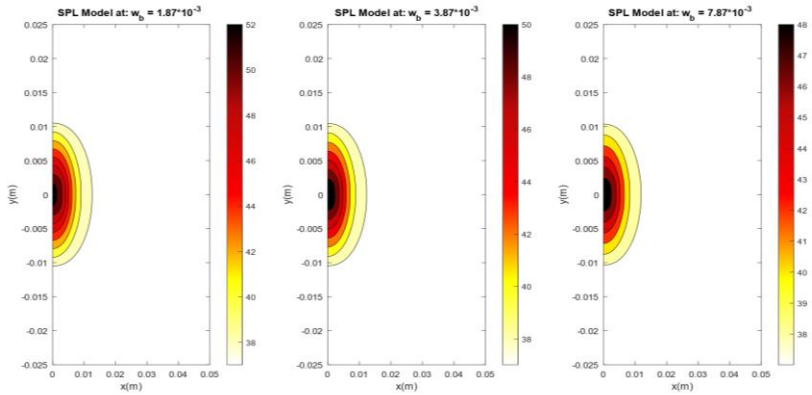

Fig. 8: The effect of the rate of the blood perfusion on contour plots of the temperature variations along with the changes in space according to SPL bio-heat model at $t = 60$s.

Figures 9-12 display the effect of the time of tissue exposure to the laser t_p on the distribution of temperature over the distance at $t = 60$s, as well as the time histories of surface temperature at $x = 0$. It is clear that the higher the time of tissue exposure to the laser, the higher the temperature. When the laser is applied to the skin too long, this leads to a rise in the temperature of the skin.

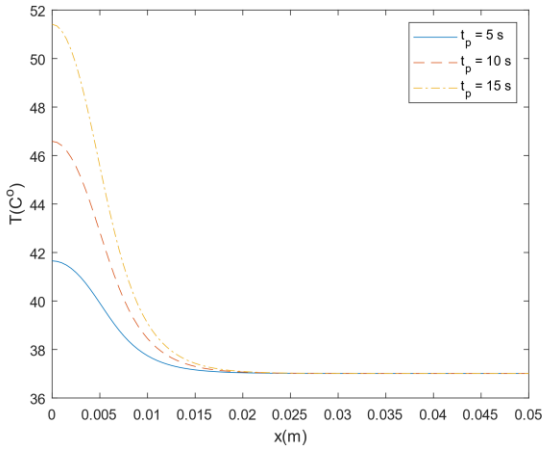

Fig. 9. The effect of the time of tissue exposure to the laser on the distribution of temperature over the distance at $y = 0$ and $t = 60$ s according to SPL bio-heat model.

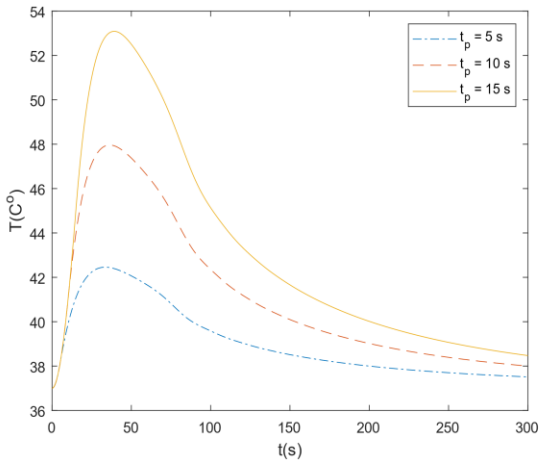

Fig. 10: The effect of the time of tissue exposure to the laser on the time histories of surface temperature at x = y= 0 according to SPL bio-heat model.

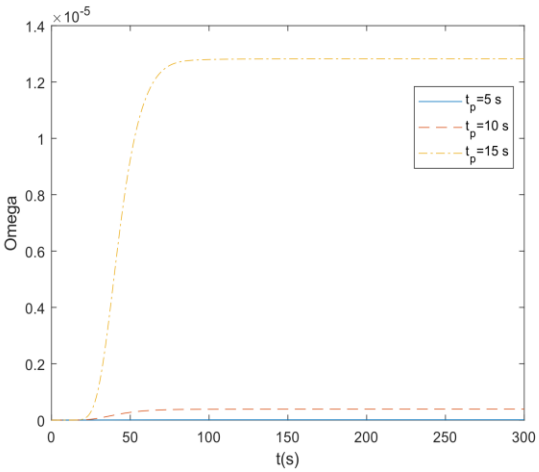

Fig. 11: The estimated thermal damage occurring to the time of tissue exposure to the laser with time on SPL bio heat models at $x = y = 0$.

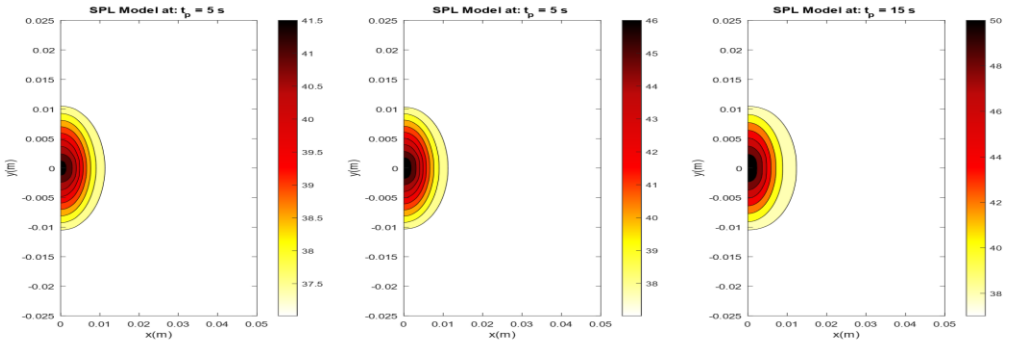

Fig. 12. The effect of the time of tissue exposure to the laser on contour plots of the temperature variations along with the changes in space according to SPL bio-heat model $t = 60$s.

Figures 13-15 display the effect of the density of the laser beam I_o on the distribution of temperature over the distance at $y = 0$ and $t = 60$s, as well as the time histories of surface temperature at $x = y = 0$.

© 2022 Sohag University

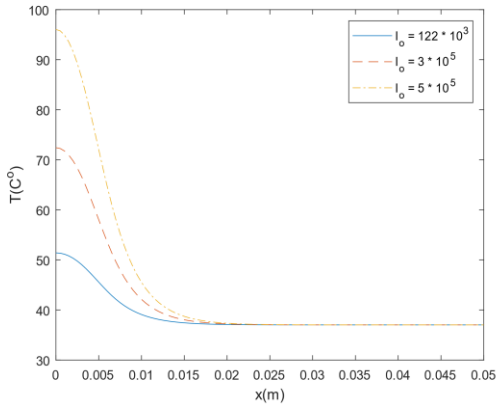

Fig. 13:. The effect of the density of the laser beam on the distribution of temperature over the distance at $t = 60$ s and $y = 0$ according to SPL bio-heat model.

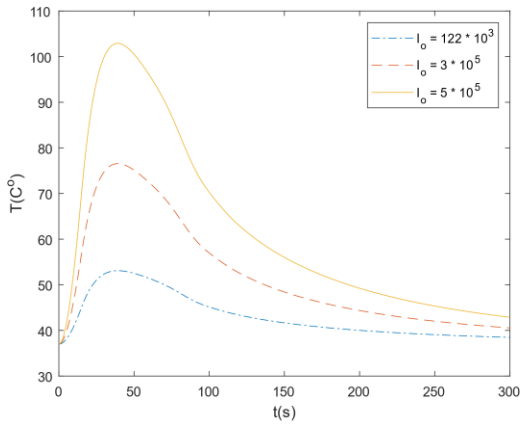

Fig. 14: The effect of the density of the laser beam on the time histories of surface temperature at $x = y = 0$ according to SPL bio-heat model.

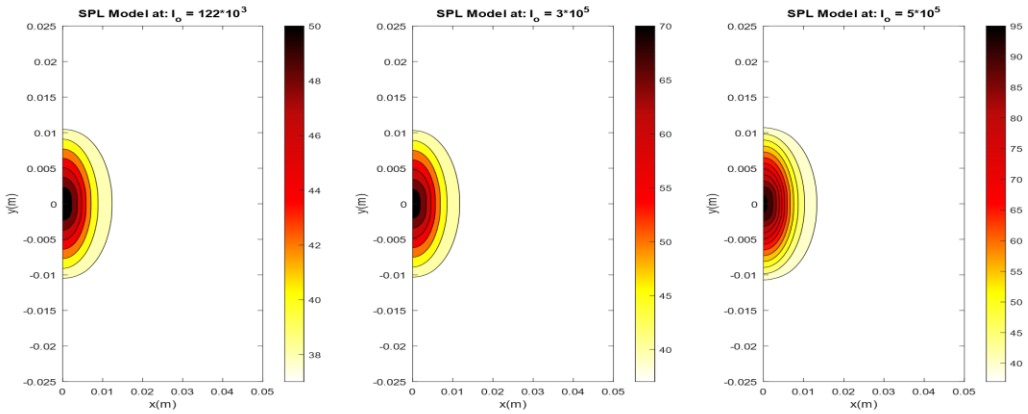

Fig. 15: The effect of the density of the laser beam on contour plots of the temperature variations along with the changes in space according to SPL bio-heat model $t = 60$s.

5. Conclusion

Based on the hyperbolic heat equation, a 2-D single phase-lag (SPL) bio-heat model has been used to estimate the variations in temperature and the thermal damage in living tissue. The model has been solved by using the alternating direction implicit (ADI) finite difference method. A comparison was also made between the Pennes model outcomes and the SPL model outcomes. The effects of laser parameters, blood perfusion, and relaxation time on heat transfer in living tissue were studied, and the results were presented graphically.

6. References

[1] Bailey, C.A., et al., Optimization of selective hyperthermia. Journal of Biomedical Optics, 2004. 9(3): p. 648-654.

[2] Pennes, H. H., Analysis of tissue and arterial blood temperatures in the resting human forearm. Journal of applied physiology, 1948. 1(2): p. 93-122.

[3] Xu, F. and T. Lu, Introduction to skin biothermomechanics and thermal pain. 2011: Springer.

[4] Richardson, A.W. and C.J. Imig, The relationship between deep tissue temperature and blood flow during electromagnetic irradiation. Archives of physical medicine and rehabilitation, 1950. 31(1): p. 19-25.

[5] Roemer, R.B., J.R. Oleson, and T.C. Cetas, Oscillatory temperature response to constant power applied to canine muscle. American Journal of Physiology - Regulatory Integrative and Comparative Physiology, 1985. 18(2): p. R153-R158.

[6] Mitra, K., et al., Experimental Evidence of Hyperbolic Heat Conduction in Processed Meat. Journal of Heat Transfer, 1995. 117(3): p. 568-573.

[7] Davydov, E., et al., Nondiffusive heat transfer in muscle tissue. Preliminary results. arXiv preprint cond-mat/0102006, 2001.

[8] Banerjee, A., et al., Temperature distribution in different materials due to short pulse laser irradiation. Heat Transfer Engineering, 2005. 26(8): p. 41-49.

[9] Cattaneo, C., A form of heat-conduction equations which eliminates the paradox of instantaneous propagation. Comptes Rendus, 1958. 247: p. 431.
[10] Vernotte, P., Les paradoxes de la theorie continue de l'equation de la chaleur. Compt. Rendu, 1958. 246: p. 3154-3155.
[11] Wahyudi, S., P. Lestari, and F. Gapsari, Application of Finite Difference Methods (FDM) on Mathematical Model of Bioheat Transfer of One-dimensional in Human Skin Exposed Environment Condition. Journal of Mechanical Engineering Research and Developments, 2021. 44(5): p. 1-9.
[12] Zhao, J. J., et al., A two level finite difference scheme for one dimensional Pennes' bioheat equation. Applied Mathematics and Computation, 2005. 171(1): p. 320-331.
[13] Patil, H. M., and R. Maniyeri, Finite difference method based analysis of bio-heat transfer in human breast cyst. Thermal Science and Engineering Progress, 2019. 10: p. 42-47.
[14] Kabiri, A. and M.R. Talaee, Analysis of hyperbolic Pennes bioheat equation in perfused homogeneous biological tissue subject to the instantaneous moving heat source. SN Applied Sciences, 2021. 3(4).
[15] Kabiri, A. and M.R. Talaee, Thermal field and tissue damage analysis of moving laser in cancer thermal therapy. Lasers in Medical Science, 2021. 36(3): p. 583-597.
[16] Alanazi, R.S. and A. Laref, Monte Carlo Simulations of the photo-thermal cancer therapy of melanin. Indian Journal of Physics, 2021. 95(12): p. 2589-2605.
[17] Abdalla, A., I. Abbas, and H. Sapoor, The effects of fractional derivatives of bio-heat model in living tissues using analytical-numerical method. Information Sciences Letters, 2022. 11(1): p. 7-13.
[18] Kabiri, A. and M.R. Talaee, Non-Fourier bioheat model for bone grinding with application to skull base neurosurgery. Proceedings of the Institution of Mechanical Engineers, Part H: Journal of Engineering in Medicine, 2022. 236(1): p. 84 - 93.
[19] Hobiny, A. and I. Abbas, Analytical solutions of fractional bioheat model in a spherical tissue. Mechanics Based Design of Structures and Machines, 2021. 49(3): p. 430-439.
[20] Ezzat, M.A. and A.A. Bary, State space approach of two-temperature magneto-thermoelasticity with thermal relaxation in a medium of perfect conductivity. International Journal of Engineering Science, 2009. 47(4): p. 618-630.
[21] Ezzat, M.A., A.A. El-Bary, and N.S. Al-Sowayan, Tissue responses to fractional transient heating with sinusoidal heat flux condition on skin surface. Animal Science Journal, 2016. 87(10): p. 1304-1311.
[22] Yasein, M., et al., The influence of variable thermal conductivity of semiconductor elastic medium during photothermal excitation subjected to thermal ramp type. Results in Physics, 2019. 15.
[23] Mahdy, A.M.S., et al., Analytical solutions of time-fractional heat order for a magneto-photothermal semiconductor medium with Thomson effects and initial stress. Results in Physics, 2020. 18.
[24] Khamis, A.K., et al., Thermal-piezoelectric problem of a semiconductor medium during photo-thermal excitation. Waves in Random and Complex Media, 2021. 31(6): p. 2499-2513.
[25] Namiki, T., A New FDTD algorithm based on alternating-Direction implicit method. IEEE Transactions on Microwave Theory and Techniques, 1999. 47(10): p. 2003-2007.
[26] Zheng, F., Z. Chen, and J. Zhang, A Finite-Difference Time-Domain Method Without the Courant Stability Conditions. IEEE Microwave and Guided Wave Letters, 1999. 9(11): p. 441-443.
[27] Zheng, F. and Z. Chen, Toward the development of a three-dimensional unconditionally stable finite-difference time-domain method. IEEE Transactions on Microwave Theory and Techniques, 2000. 48(9): p. 1550-1558.
[28] Xu, F., et al., Mathematical modeling of skin bioheat transfer. Applied Mechanics Reviews, 2009. 62(5): p. 1-35.
[29] Mitchell, J.W., et al., Thermal response of human legs during cooling. Journal of Applied Physiology, 1970. 29(6): p. 859-865.
[30] Gardner, C.M., S.L. Jacques, and A.J. Welch, Light transport in tissue: Accurate expressions for one-dimensional fluence rate and escape function based upon Monte Carlo simulation. Lasers in Surgery and Medicine, 1996. 18(2): p. 129-138.
[31]Vernardou, D., et al., Hydrothermal Growth of MnO2 at 95 oC as an Anode Material. International Journal of Thin Film Science and Technology, 2016. 5(2): p. 7.
[32] S Al-Qrinawi, M., et al., Capacitance-voltage measurements of hetero-layer OLEDs treated by an electric field and thermal annealing. International Journal of Thin Film Science and Technology, 2021. 10(3): p. 11.
[33] Elhadary, A.A., et al., Studying the effect of the dielectric barrier discharge non-thermal plasma on colon cancer cell line. International Journal of Thin Film Science and Technology, 2021. 10(3): p. 161-168.
[34] Shapaan, M., DC Conductivity, Thermal Stability and Crystallization Kinetics of the Semiconducting

© 2022 Sohag University

30P2O5 (50-x) V2O5 xB2O3 20Fe2O3 Oxide Glasses. International Journal of Thin Film Science and Technology, 2016. 5(3): p. 1.
[35] Askarizadeh, H. and H. Ahmadikia, Analytical analysis of the dual-phase-lag model of bioheat transfer equation during transient heating of skin tissue. Heat and Mass Transfer/Waerme- und Stoffuebertragung, 2014. 50(12): p. 1673-1684.
[36] Henriques Jr, F. and A. Moritz, Studies of thermal injury: I. The conduction of heat to and through skin and the temperatures attained therein. A theoretical and an experimental investigation. The American journal of pathology, 1947. 23(4): p. 530.
[37] Moritz, A.R. and F.C. Henriques, Studies of Thermal Injury: II. The Relative Importance of Time and Surface Temperature in the Causation of Cutaneous Burns. The American journal of pathology, 1947. 23(5): p. 695-720.
[38] Dombrovsky, L. and V. Timchenko, Laser induced hyperthermia of superficial tumors: computational models for radiative transfer, combined heat transfer, and degradation of biological tissues. Therm Process Eng, 2015. 7(1): p. 24-36.
[39] Johnson, J.M. and M.K. Park, Reflex control of skin blood flow by skin temperature: Role of core temperature. Journal of Applied Physiology Respiratory Environmental and Exercise Physiology, 1979. 47(6): p. 1188-1193.